12th IFAC International Symposium on
Advanced Control of Chemical Processes
July 14-17, 2024. Toronto, Canada

Reliability-based Optimal Control of Crystallization Systems Under Uncertainty

Yash Barhate*, Zoltan K. Nagy*

**Davidson School of Chemical Engineering, Purdue University, 480 W Stadium Ave, West Lafayette, IN, 47907, USA (e-mail: znagy@purdue.edu)*

Abstract: Population balance model-based approaches have become ubiquitous in crystallization process design and control to drive crystallization systems to meet the required industry-specific critical quality attributes (CQAs). However, the reliability of model-based approaches is often subject to uncertain model parameters, which are usually determined through parameter estimation routines that process noisy experimental data. Disregarding these uncertainties during design often results in unexpected operational failures, suboptimal performance, or failure to attain desired CQAs. In this study, a reliability-based design optimization (RBDO) framework was applied for the open-loop control design of crystallization processes under parametric uncertainty. First, the concept of reliability-based design optimization was introduced to design crystallization systems under uncertainty to meet the target CQAs with a desired probability. A nested two-level simulation-optimization approach using surrogate modeling was used to solve RBDO problems. Finally, the above method was applied to demonstrate its effectiveness using a case study for batch crystallization process design. The results show that the RBDO-based approach provides reliable open-loop setpoint trajectories with higher probabilities of satisfying the desired CQAs when compared with open-loop optimization using nominal model parameters.

Keywords: optimization under uncertainty, crystallization, optimal control, reliability-based design optimization, parameter uncertainty, continuous crystallization, pharmaceutical manufacturing

1. INTRODUCTION

Crystallization is an integral purification and particle attribute control unit operation in the manufacturing processes of several industries, including pharmaceuticals, specialty chemicals, and energetics (Mullin, 2001). The properties of the crystals produced during the crystallization step not only impact the attributes of the final product but also the downstream manufacturing steps post-crystallization. Typically, crystallization processes are designed to consistently produce crystals that meet the desired Critical Quality Attributes (CQAs) such as purity, yield, and crystal size distribution (CSD). The values of the different target CQAs are usually determined based on the trade-off between specific product attributes. For instance, in the pharmaceutical industry, crystal size distribution is a crucial CQA, and its target range is determined through a trade-off between the drug's bioavailability and its manufacturability (Kirwan and Orella, 2002). Therefore, the goal of the crystallization process design is to find optimal trajectories within the design space that enable the consistent production of crystals meeting the target CQAs.

Model-based design approaches have shown immense potential in achieving the above-mentioned goal in a resource-efficient manner (Fujiwara *et al.*, 2005). However, because the model parameters in these approaches are determined through parameter estimation methods that process noisy experimental data, ignoring the uncertainty associated with these parameters during optimal control and design can hinder the effectiveness of model-based results. Implementing optimal trajectories obtained without considering parameter uncertainty in experimental settings may lead to unexpected operational failures, suboptimal performance, or failure to meet the target CQAs (Xie and Schenkendorf, 2019). Hence, several efforts have been made in the literature to design and control processes under uncertainty. Within this context, three prominent branches emerge, namely Multi-stage stochastic optimization, Robust optimization, and Chance Constrained Programming (Sharifian *et al.*, 2021).

Reliability-based design optimization (RBDO) is an application of chance-constrained programming. Unlike generic chance-constrained programming, RBDO formulations exclusively consider deterministic design variables in the objective function, thus avoiding the next to relax the objective function under uncertainty. Unlike robust optimization, which pursues designs with high degrees of robustness by enforcing conservative design choices that minimize sensitivity to parameter uncertainties, RBDO provides flexibility to quantify system failure probabilities. It aims to derive optimal designs that ensure the satisfaction of probabilistic constraints at user-specified levels, effectively achieving a trade-off between robustness and the associated design cost required to attain resilience against model parameter uncertainties (Acar *et al.*, 2021; Libotte *et al.*, 2022). While RBDO has been extensively studied in the field of structural design optimization, with a few recent applications in chemical engineering, its potential application and effectiveness in crystallization process design and control is unexplored (Moustapha and Sudret, 2019; Libotte *et al.*, 2022). The primary objective of this paper is to bridge this knowledge gap and demonstrate the applicability of RBDO in

the context of open-loop optimal control of crystallization systems under uncertainty.

2. RELIABILITY BASED DESIGN OPTIMIZATION

A generic reliability-based design optimization problem formulation can be represented as follows,

$$\min c(\boldsymbol{d}) \qquad (1)$$

$$subject\ to\ f_j(\boldsymbol{d}) \leq 0 \qquad \{j = 1, \dots, s\}$$

$$\mathcal{P}(g_k(\boldsymbol{d}, \boldsymbol{x}, \boldsymbol{\theta}) \leq 0) \leq \mathcal{P}_{f_k} \qquad \{k = 1, \dots, n\}$$

where the objective is to minimize the cost function $c(\boldsymbol{d})$ with respect to the decision variables $\boldsymbol{d} \in \mathbb{D}$. The formulation involves a combination of hard constraints, which are always satisfied (i.e., $f_j(\boldsymbol{d}) \leq 0$), and soft constraints that are modeled as probabilistic constraints. The system is considered to be in a state of failure for any $\boldsymbol{d}$ when the condition $g_k(\boldsymbol{d}, \boldsymbol{x}, \boldsymbol{\theta}) \leq 0$ is satisfied. Here, $\boldsymbol{x} = \boldsymbol{x}(\boldsymbol{d}, \boldsymbol{\theta}) \in \mathbb{X}$ is a vector of state variables and $\boldsymbol{\theta} \in \boldsymbol{\Theta}$ is a vector of uncertain model parameters represented by the joint probability distribution $\boldsymbol{\Theta}$**.** In RBDO, the probabilistic constraints necessitate that all failure probabilities $\mathcal{P}(g_k(\boldsymbol{d}, \boldsymbol{x}, \boldsymbol{\theta}) \leq 0)$ are less than a user-defined threshold probability $\mathcal{P}_{f_k}$. Hence, this formulation provides a higher degree of flexibility during control design under uncertainty compared with robust optimization formulations.

Typically, specific target ranges are defined for various CQAs of crystallization products based on trade-offs between different factors related to product characteristics and manufacturability. The crystallization system can be considered to be in a state of failure if, for any given design, the output CQAs deviates from the acceptable target range. In the context of open-loop crystallization control design under parametric uncertainty, probabilistic constraints can be established based on the probability of not achieving the desired targets for CQAs under uncertainty. Furthermore, hard constraints can be applied to design trajectories to ensure operational feasibility, with the optimization objective centered on maximizing process productivity.

3. SYSTEMATIC FRAMEWORK FOR SOLVING RBDO PROBLEMS USING SURROGATE MODELING

In this study, a nested two-level simulation-optimization approach was employed to solve the generalized RBDO problem represented in equation (1). Here, the outer loop explores the design space, while the inner loop calculates the corresponding failure probabilities $\mathcal{P}(g_k(\boldsymbol{d}, \boldsymbol{x}, \boldsymbol{\theta}) \leq 0)$ for each design $\boldsymbol{d}$**.** Within the inner loop, failure probabilities were computed using the Monte Carlo-based sample average approximation (SAA) method. This involves approximating the multivariate integration of the joint probability density function of the random variable over the failure domain $g_k(\boldsymbol{d}, \boldsymbol{x}, \boldsymbol{\theta}) \leq 0$, by a discrete sample-based estimate (Pagnoncelli, Ahmed and Shapiro, 2009). Despite being computationally intensive due to the need for multiple sample evaluations, the above method has a well-characterized convergence behavior that enables confidence bounds to be calculated for the failure probability estimates (Rubinstein and Kroese, 2016).

To overcome the high computational costs associated with the need for a large number of samples to achieve a good approximation coupled with the cost of computing expensive high-fidelity models, surrogate modeling was used to reduce the computational cost by substituting expensive high-fidelity models with inexpensive-to-evaluate surrogates (Nagy and Braatz, 2007; Makrygiorgos, Maggioni and Mesbah, 2020). In the context of RBDO, surrogate models are built within a trust region to approximate the failure constraints $g_k \leq 0$ by augmenting both the deterministic design and uncertain parametric spaces. This approach circumvents the need to repeatedly construct surrogate models from scratch for each design iteration within the outer optimization loop, thus reducing computational overhead. Having accurate surrogate models for representing the failure domain is essential in this approach, since inaccuracies in surrogate models may result in either underestimation or overestimation of failure probabilities, leading to sub-optimal RBDO solutions. Since building a surrogate model that is globally accurate is challenging, active learning with adaptive sampling was used to enhance the accuracy of surrogate model in regions of interest such as the failure domain $g_k \leq 0$ (Moustapha and Sudret, 2019). The typical flow for solving problem (1) is summarized in the flowchart shown in figure 1 and was implemented using UQLab (Marelli and Sudret, 2014).

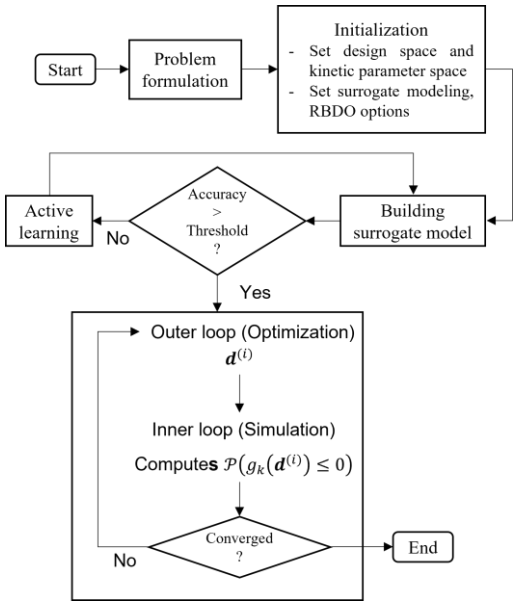

Figure 1: Solution methodology used for solving RBDO problems.

4. CASE STUDY: OPEN-LOOP CONTROL USING RBDO FOR A BATCH CRYSTALLIZATION PROCESS

In this case study, the proposed framework is applied to the optimal open-loop control design of batch cooling crystallization of a commercial active pharmaceutical ingredient (API), diphenhydramine hydrochloride (DPH).

4.1 Mathematical model development

In this section, the model equations comprising the high-fidelity population balance model (PBM) for describing the

batch crystallization dynamics of DPH in isopropyl alcohol (IPA) are presented. Population balance equation (2) tracks the crystal number density (f) in the batch crystallizer with respect to time (t) and crystal length (L), under primary nucleation, secondary nucleation, size-dependent growth, and agglomeration mechanisms.

$$\frac{\partial f(t,L)}{\partial t}+\frac{\partial (G(L)f(t,L))}{\partial L} = [B_p + B_s]\delta(L-L_m) + \frac{1}{2}\int_0^L \beta(t,L-\lambda,\lambda)f(t,L-\lambda)f(t,\lambda)d\lambda - \int_0^\infty \beta(t,L,\lambda)f(t,L)f(t,\lambda)d\lambda \quad (2)$$

Equation (2) is subjected to the following initial condition characterizing the initial crystal size distribution, along with the following boundary condition that limits the growth of all crystals to a finite size.

$$f(L,t=0) = f_0(L) \qquad \lim_{L\to\infty} f(L) = 0 \quad (3)$$

Equation (2) is coupled with a mass balance equation that tracks the solute concentration (c) in the crystallizer, as shown below:

$$\frac{\mathrm{d}c}{\mathrm{d}t} = -\frac{k_v\rho_c}{\rho_s 10^{18}}\left[3\int_0^\infty GL^2 f(L,t)\,\mathrm{d}L + \left(B_p + B_s\right)L_m^3\right] \quad (4)$$

The initial condition for equation (4) is $c(t=0)=c_0$, where c_0 represents the initial concentration (g solute/g solution) in the batch crystallizer. Table 1 shows the other supplementary equations required to complete the PBM model description.

Table 1: Supplementary equations describing various crystallization mechanisms

Mechanism	Equation
Supersaturation	$\sigma = \frac{C - C_s}{C_s}$
Solubility	$C_s(\frac{g\ solute}{g\ solvent}) = exp\left[A + \frac{B}{T\ (K)} + C\ ln(T\ (K))\right]$
Primary Nucleation	$B_p(\#m^{-3}s^{-1}) = k_p\sigma^p$
Secondary Nucleation	$B_s(\#m^{-3}s^{-1}) = k_s\sigma^s V_c$
Volume fraction of crystals	$V_c = k_v\int_0^\infty L^3 f(L)dL$
Size dependent growth	$G\ (\mu m.s^{-1}) = k_g(\beta L^\gamma)\sigma^g exp\left(\frac{-E_g}{RT}\right)$
Agglomeration	$\beta(L,\lambda)\ (m^3 s^{-1}\#^{-1}) = k_{agg}$

The values of the parameters used in the above model are listed in Table 2 below.

Table 2: Values of different constants and kinetic parameters

Parameter	Value	Units
k_v	0.52	-
ρ_c	1048.9	kg/m^3
ρ_{sol}	782	kg/m^3
A	51.17	-
B	-8155	-
C	-4.695	-
$\log(k_p)$	8.2139 ± 0.367	#/m^3. s
$\log(k_s)$	11.151 ± 0.367	#/m^3. s
$\log(k_g)$	5.8029 ± 0.5059	µm/s
β_g	1.43 ± 0.0106	µm^{-1}
$\log(k_{agg})$	-17.3385 ± 0.2293	#/m^3. s
p	2.5	-
s	1.5	-
g	1.1	-
γ_g	0.5222	-
E_g	45	kJ/mol

The PBM model and the corresponding uncertain model parameters presented here were experimentally estimated and validated, with further details available elsewhere (Barhate *et al.*, 2024).

4.2 RBDO formulation and solution methodology

During a typical batch cooling crystallization process, the implemented temperature trajectory influences the generated supersaturation driving force in the crystallizer. This further affects the attributes of products (CQAs) obtained at the end of the batch. Hence, for a batch cooling crystallization open-loop control design, the following optimization problem can be formulated,

$$\min_{T_1,T_2,T_3,T_4,t_{batch}} t_{batch} \quad (5)$$
$$subject\ to\ -1 \le \frac{dT}{dt} \le -0.1$$
$$150 < Mean\ size$$
$$Mean\ size < 350$$
$$50 < SD$$
$$SD < 150$$
$$T_i(^\circ C) \in [10,48],\ t_{batch}(min) \in [35,120]$$

Here, the objective is to optimize the temperature trajectory to minimize the overall batch time while ensuring that the product CQA's, represented by the volumetric mean size ($Mean\ size$) and standard deviation (SD) of CSD, remain within predetermined target ranges. The constraints on $Mean\ size$ and SD are terminal constraints, enforced at the end of the batch when their measurement will be available using offline characterization tools. To facilitate computation, the temperature-time trajectory is discretized into four equidistant temperature points relative to the overall batch time, thus transforming the problem from infinite-dimensional to finite-dimensional. Additionally, an operational feasibility constraint is imposed by limiting the cooling rate to fluctuate

between -0.1 to -1°C/min. This constraint is enforced discretely on the temperature trajectory by ensuring that the temperature differentials between successive points fall within the specified bounds. The definitions of $Mean\ size$ and SD are given in Equations (6) and (7), respectively.

$$Mean\ size = \frac{\int_0^\infty L^4 f(L)dL}{\int_0^\infty L^3 f(L)dL} \quad (6)$$

$$SD = \sqrt{\frac{\int_0^\infty L^2 f_{vf}(L)dL}{\int_0^\infty f_{vf}(L)dL} - \left(\frac{\int_0^\infty L f_{vf}(L)dL}{\int_0^\infty f_{vf}(L)dL}\right)^2} \quad (7)$$

Here, $f_{vf}(L)$ denotes the volume-based crystal size distribution [$f_{vf}(L) = k_v L^3 f$].

The open loop setpoint obtained by solving the above problem is sensitive to the accuracy of the kinetic model parameters because their uncertainty has not been incorporated in the problem formulation. While designing under parametric uncertainty, the above problem can be re-formulated using the RBDO framework as follows,

$$\min_{T_1,T_2,T_3,T_4,t_{batch}} \quad t_{batch} \quad (8)$$

$$subject\ to\ -1 \le \frac{dT}{dt} \le -0.1$$
$$\mathcal{P}[(150 - Mean\ size) < 0] \le \mathcal{P}_{f1}$$
$$\mathcal{P}[(Mean\ size - 350) < 0] \le \mathcal{P}_{f2}$$
$$\mathcal{P}[(50 - SD) < 0] \le \mathcal{P}_{f3}$$
$$\mathcal{P}[(SD - 150) < 0] \le \mathcal{P}_{f4}$$
$$\boldsymbol{\theta} \in \boldsymbol{\Theta}, T_i(^\circ C) \in [10,48], t_{batch}(min) \in [35, 120]$$

In this formulation, process failure is defined when the product CQA's fall out of the acceptable range, and hence, are modeled as probabilistic constraints, thereby allowing user flexibility in defining the necessary failure probability thresholds for each of the constraints based on their relative importance. This flexibility prevents the overcompensation of the optimal temperature trajectory under parametric uncertainty. The utilization of single chance constraints, rather than joint chance constraints, offers greater flexibility in specifying threshold failure probabilities. This strategy is particularly advantageous in pharmaceutical crystallization applications, where constraints related to bioavailability may carry greater significance compared to others, such as manufacturability. By employing single-chance constraints, distinct failure probabilities can be assigned to individual bounds, facilitating tailored risk management.

In this study, sparse-polynomial chaos expansion (s-PCE) was selected as a surrogate model to approximate the nonlinear PBM model based on both literature survey and preliminary in silico investigations (Nagy and Braatz, 2007; Makrygiorgos, Maggioni and Mesbah, 2020). The general form of s-PCE model is represented as

$$Y \approx M^{PCE}(\boldsymbol{X}) = \sum_{\alpha \epsilon A} c_\alpha \psi_\alpha(\boldsymbol{X}) \quad (9)$$

Here, multivariate polynomials $\psi_\alpha(\boldsymbol{X})$ are employed as basis functions, with c_α representing the coefficients associated with these basis functions. Least-angle-regression (LAR) algorithm is used to identify polynomials exerting the most significant impact on the model responses from a large pool of candidates using the hyperbolic truncation scheme (Blatman and Sudret, 2011; Makrygiorgos, Maggioni and Mesbah, 2020).

The kinetic parameter space was assumed to follow a multivariate normal distribution with independent parameters. Table 2 provides the nominal values and 95% confidence interval values for these uncertain parameters. First, the kinetic and design parameter spaces were augmented, and comprehensive global surrogate models were constructed for each constraint using N = 9066 sample points. While constructing the s-PCE models, a hyperbolic truncation scheme with q = 0.75 was used and the degrees of basis functions were restricted to range from 2 to 5. The surrogate models were also validated on a test dataset where the percentage prediction error was found to be less than 5 %, before using them in the RBDO framework. To address the non-convexity of the RBDO problem and the challenges associated with computing gradients of probabilistic constraints, the derivative-free constrained covariance matrix adaption evolution strategy (C-CMAES) algorithm was selected for the outer optimization loop (Arnold and Hansen, 2012). The computation of failure probabilities for all constraints was performed in the inner loop, as detailed in Section 3. The computational burden associated with a derivative-free solver remains moderate, primarily since the cost function in RBDO problems is typically a simple analytical function, and the failure probability estimation relies on inexpensive-to-evaluate surrogate models. This solution methodology enhances the overall computational tractability of solving RBDO problems. The only computational bottleneck in the aforementioned surrogate-based approach lies in constructing accurate surrogate models to approximate failure domains. However, once developed, these surrogate models enable the solution of underlying RBDO problems within seconds, across various threshold failure probabilities.

4.3 Results and discussion

RBDO problem (8) was solved for different values of the threshold failure probabilities $\mathcal{P}_{f_k}$(0.5, 0.2, 0.15, and 0.1). Although different threshold probabilities can be specified for each constraint corresponding to different CQAs, here same threshold values were assigned to all constraints. The optimization problem returned a converged solution for all the above cases, except for $\mathcal{P}_{f_k} = 0.1$. In this case, the optimizer could not identify any temperature trajectory that ensured the failure probability of constraints to be less than 0.1 for the

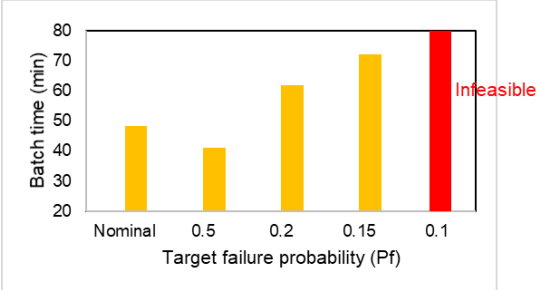

Figure 2: Threshold failure probability (reliability) versus batch time (productivity).

considered uncertainty space. To make the solution feasible at a threshold probability of 0.1, one either has to relax the acceptable region bounds on the CQA's or obtain more precise kinetic parameter estimates with less uncertainty. In the case study, the approximation error of the surrogate model had no impact on the feasibility of optimization results. This was validated by comparing failure probabilities for all optimal designs computed using surrogate models and with those computed from expensive PBM models. The computed failure probabilities were comparable across all constraints and consistently stayed below the specified threshold failure probabilities.

Figure 2 illustrates a bar graph that presents the final objective function values for each problem, corresponding to different threshold failure probabilities. In addition, these solutions were compared with the nominal solution obtained for problem (5), where the parameter uncertainty was ignored. As the threshold failure probability increased, making the process more reliable, a concomitant increase in batch time was observed. Hence, a tradeoff exists between the desired reliability and the design cost in terms of the process batch time required to achieve that reliability.

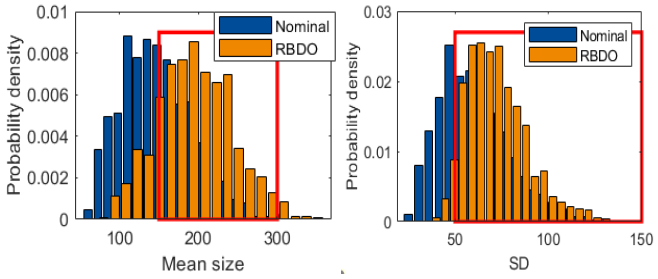

Figure 3: Probability distributions of mean size and standard deviation of CSD for nominal and RBDO solution with threshold probability failure of 0.15.

Figure 3 presents a comparison of the probability distributions of $Mean\ size$ and SD for both the nominal solution and RBDO solution with $\mathcal{P}_{f_k} = 0.15$. It can be clearly seen, that as expected, the nominal solution has approximately 50% of distribution outside the acceptable region marked by red box, however the RBDO solution has less than 15 % of its distribution falling outside the acceptable region on either side, making the process more reliable. Thus, implementing the optimal open-loop control trajectory obtained from the RBDO solution will increase the process robustness and help minimize the plant-model mismatch due to parameter uncertainty.

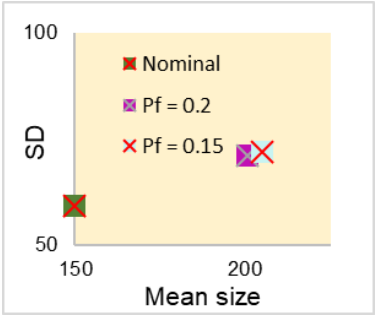

Figure 4: Nominal and RBDO solutions obtained at various threshold failure probabilities.

Figure 4 offers a bird's-eye view comparison between the nominal and RBDO solutions along the boundaries of the specified range of CQAs. The nominal solution, derived without factoring in parameter uncertainty, aligns with the boundaries of the acceptable CQAs, presenting a trajectory with the minimum batch time. However, as this solution resides at the boundaries, even a slight deviation in the values of the kinetic parameters could potentially propel the solution beyond the target region, leading to process failure. The RBDO formulation addresses this vulnerability by ensuring that the solution is positioned within the feasible region such that the process failure risk is less than the desired threshold levels at the expense of a slightly longer batch time.

6. CONCLUSIONS

This study presents a population balance model-based design framework for optimal open-loop control design in crystallization processes, integrating kinetic parameter uncertainty through reliability-based design optimization (RBDO). RBDO formulations were applied to a batch crystallization control design case study, aiming to determine setpoint temperature trajectories that guarantee the fulfillment of product CQAs within the target range under parametric uncertainty. The employed solution methodology utilizes a nested two-level simulation-optimization approach with sparse-polynomial chaos expansions used as surrogate models. The results highlight that the RBDO-based approach yields robust open-loop trajectories with higher probabilities of meeting the specified CQAs under uncertainty compared with open-loop optimization using nominal parameters. However, this enhanced reliability is accompanied by an increase in batch time, introducing a tradeoff between the desired robustness and the associated design cost needed to achieve it. The proposed approach effectively quantifies the risk probability associated with the control design and optimizes it while ensuring the risk/failure probabilities remain below the user-specified thresholds given model parameter uncertainties.

ACKNOWLEDGEMENTS

Funding for this work was made possible, by the US Food and Drug Administration (FDA) through grant number 75F40121C00106. Views expressed herein do not necessarily reflect the official policies of the Department of Health and Human Services; nor does any mention of trade names, commercial practices, or organizations imply endorsement by the United States Government.

REFERENCES

Acar, E. *et al.* (2021) 'Modeling, analysis, and optimization under uncertainties: a review', *Structural and Multidisciplinary Optimization 2021 64:5*, 64(5), pp. 2909–2945.

Arnold, D. V. and Hansen, N. (2012) 'A (1+1)-CMA-ES for constrained optimisation', *GECCO'12 - Proceedings of the 14th International Conference on Genetic and Evolutionary Computation*, pp. 297–304.

Barhate, Y. *et al.* (2024) 'Population balance model enabled digital design and uncertainty analysis framework for continuous crystallization of pharmaceuticals using an automated platform with full recycle and minimal material use', *Chemical Engineering Science*, 287, p. 119688.

Blatman, G. and Sudret, B. (2011) 'Adaptive sparse polynomial chaos expansion based on least angle regression', *Journal of Computational Physics*, 230(6), pp. 2345–2367.

Fujiwara, M. *et al.* (2005) 'First-principles and direct design approaches for the control of pharmaceutical crystallization', *Journal of Process Control*, 15(5), pp. 493–504.

Kirwan, D.J. and Orella, C.J. (2002) 'Crystallization in the pharmaceutical and bioprocessing industries', in *Handbook of Industrial Crystallization*. Butterworth-Heinemann, pp. 249–266.

Libotte, G.B. *et al.* (2022) 'A Novel Reliability-Based Robust Design Multiobjective Optimization Formulation Applied in Chemical Engineering', *Industrial and Engineering Chemistry Research*, 61(9), pp. 3483–3501.

Makrygiorgos, G., Maggioni, G.M. and Mesbah, A. (2020) 'Surrogate modeling for fast uncertainty quantification: Application to 2D population balance models', *Computers & Chemical Engineering*, 138, p. 106814.

Marelli, S. and Sudret, B. (2014) 'UQLab: A Framework for Uncertainty Quantification in Matlab', *Vulnerability, Uncertainty, and Risk: Quantification, Mitigation, and Management - Proceedings of the 2nd International Conference on Vulnerability and Risk Analysis and Management, ICVRAM 2014 and the 6th International Symposium on Uncertainty Modeling a*, pp. 2554–2563.

Moustapha, M. and Sudret, B. (2019) 'Surrogate-assisted reliability-based design optimization: a survey and a unified modular framework', *Structural and Multidisciplinary Optimization*, 60(5), pp. 2157–2176.

Mullin, J.W. (John W. (2001) 'Crystallization', p. 594.

Nagy, Z.K. and Braatz, R.D. (2007) 'Distributional uncertainty analysis using power series and polynomial chaos expansions', *Journal of Process Control*, 17(3), pp. 229–240.

Pagnoncelli, B.K., Ahmed, S. and Shapiro, A. (2009) 'Sample average approximation method for chance constrained programming: Theory and applications', *Journal of Optimization Theory and Applications*, 142(2), pp. 399–416.

Rubinstein, R.Y. and Kroese, D.P. (2016) *Simulation and the Monte Carlo method*.

Sharifian, S. *et al.* (2021) 'Uncertainty in chemical process systems engineering: a critical review', *Reviews in Chemical Engineering*, 37(6), pp. 687–714.

Xie, X. and Schenkendorf, R. (2019) 'Stochastic back-off-based robust process design for continuous crystallization of ibuprofen', *Computers & Chemical Engineering*, 124, pp. 80–92.